Elastic strains and associated inelastic properties of earth crust around greater Cairo as deduced from GPS measurements

Gamal S. El-Fiky
National Research Institute of Astronomy and Geophysics, Helwan, Cairo, Egypt
gamal_elfiky@yahoo.com

To estimate the elastic and inelastic strains in and around the Cairo City, Egypt, five years of Global Positing System (GPS) measurements from 1996 to 2000 were used. The GPS data were processed using the GAMIT and GLOBK software to produce the displacement vectors of each GPS site. The Least-Squares Prediction technique (LSP) was applied to segregate the signal and noise in the observed velocity vectors. Estimated signals (displacement vectors) were differentiated in space to reconstruct the total strains (elastic plus inelastic). Then, we estimated inelastic strains of the studied region using the inversion method. The estimated rate of inelastic strains is of the order of 10^{-3} μstrains/yr. Comparing this with the rate of total strains of the order of 0.1 μstrains/yr, inelastic part was found to be negligible. Thus, shear stresses at the surface of Cairo region have been estimated based on the elastic theory. Principal axes of the stresses indicate that the compression force acting at the convergent plate boundary between the Eurasian and the African plates affect the southern part of the Nile Delta. Maximum shear stresses show two maxima of high values of stress in the northern and southern parts of the studied region separated by a very low zone of stresses or almost stress-free zone in the middle of the region. The October 12, 1992 earthquake occurred at the southern edge of this low area. This indicated that, the accumulated stresses in this low zone were almost released by the co-seismic and the post-seismic of the October 1992 earthquake. In addition, the present analysis shows that there is no evidence for earthquake activity in this low zone in the near future. This low zone of stresses has been confirmed by seismic data.

باستعمال بيانات خمس سنوات من أرصاد النظام العالمى لتحديد المواقع والمعروف باسم (GPS) تم تحديد الانفعالات المرنة والانفعالات غير المرنة حول مدينة القاهرة الكبرى. فى البداية تم تحليل بيانات (GPS) باستعمال برنامج GAMIT وبرنامج GLOBK وذلك لحساب معدل الازاحة عند كل نقطة من نقاط شبكة الرصد. بعد ذلك تم استعمال طريقة أقل التربيعات المتوقعة لفصل الازاحة الفعلية عن الأخطاء المصاحبة لها. ثم بالتفاضل الفراغى لهذه الازاحة تم حساب مجموع الانفعالات الكلية (المرنة وغير المرنة) لمنطقة الدراسة. وبعد ذلك وباستعمال طريقة النظرية العكسية لقيم الانفعالات الكلية تم حساب الانفعال غير المرن الموجود للمنطقة. ولقد أظهرت التحليلات السابقة أن قيمة الانفعال غير المرن فى حدود ١% فقط من قيمة الانفعال الكلى ولذا يمكن إهمال قيمة الانفعال غير المرن بمنطقة الدراسة بالمقارنة بالانفعال الكلى. ومن ثم يمكن حساب الاجهادات الموجودة بالمنطقة باستعمال نظرية المرونة مباشرة. ولقد أشارت النتائج إلى وجود ضغوط إجهادية فى منطقة شمال القاهرة وجنوب الدلتا والتى يمكن اعتبارها نتيجة للضغوط الناتجة من إنزلاق الصحيفة الأفريقية تحت الصحيفة الأوروبية. ولقد وضح من توزيع القص الإجهادى الأعظم أن هناك قيمة عظمى فى الجزء الشمالى وفى الجزء الجنوبى من منطقة الدراسة. وفى الجزء الأوسط يوجد قيمة دنيا من الإجهاد القصى. وقد تطابقت هذه النتائج مع بيانات الزلازل المسجلة لمنطقة الدراسة. وكذلك وجد ان مركز زلزال دهشور ١٩٩٢ قد حدث فى منطقة الاجهاد الدنيا وهذا يدل على ان هذا الزلزال قد ادى الى اطلاق معظم الاجهاد المختزن فى هذه المنطقة.

Keywords: Elastic strains, Inelastic deformation GPS data, Cairo network, Least-squares prediction

1. Introduction

The Cairo region has been the focus of intense geological and geophysical investigations since the occurrence of the 12th October 1992 earthquake (M_b=5.9). This moderate earthquake occurred at Dahshour city, about 25 km southwest of Cairo. In spite of its relatively moderate magnitude, it caused a widespread damage in Cairo city and its surrounding areas. It was the largest earthquake in northern Egypt in the past hundred years. Therefore, the National Research Institute of Astronomy and Geophysics (NRIAG), Egypt, started a series of geophysical studies in the epicenter area and

in and around Cairo to help understanding the physical process of the crust in this tectonically active area [1]. In addition, historical records indicated that there were two moderate but destructive earthquakes that occurred in 1303 and 1847 near to the epicenter of the 1992 earthquake [2,3]

Monitoring of crust strain fluctuations is very important to understand the physical processes in the crust as well as the prediction of crust activity. Dense Global Positing System (GPS) measurements could provide a powerful tool for monitoring crust strain. For this purpose the NRIAG has installed a GPS network consists of 11 sites, fig. 1, at the area around greater Cairo, in 1995, after the occurrence of the October 12, 1992 earthquake. In this study we used the GPS measurements from this network in and around the Cairo region for the period from 1996 to 2000, and applied the Least-Squares Prediction (LSP) technique to delineate the crust elastic and inelastic strains of this tectonically active region.

One problem in providing the strain field using geodetic data is due to the assumption that the surface crust deforms only elastically in time and our inability to detect the inelastic properties of the crust that may be relevant to earthquake prediction. Evidences from geological and geomorphologic studies in many areas suggest that the crust deformation is not purely elastic, especially for long time intervals. Thus, the estimation of the inelastic properties of the crust is important to collaborate the deformation with geomorphology. Moreover, the estimate of stresses in the crust are important in relation to earthquake occurrence, for which we need to know the inelastic deformation embedded in the total deformation. Therefore, a more appropriate way is to model the studied region as elasto-plastic bodies assuming that inelasticity comes from plastic strain. Then, the surface strains can be inverted to study the inelastic properties of the crust. This could help us to delineate elastic crust-strains after removal of the inelastic part.

In the present study, we first estimated the total strains and then, the principal components of these strains were inverted, using the inverse method proposed by [4] to study the inelastic properties of the crust in and around Cairo. Then, crust stresses in this active tectonically region are delineated from elastic crust-strains. Finally, a brief discussion of the tectonic implications of the results is given.

2. GPS measurements

GPS techniques have been extensively developed and used for crust deformation researches since the beginning of the 1980s in various regions of the world. In and around Cairo, GPS measurements were initiated early in 1996. A GPS network consists of 11 sites, fig. 1, has been established at the area around greater Cairo, in 1995, after the occurrence of the October 12, 1992 earthquake to study the crust deformation in this important area. The Nile River runs in the middle of this network, the northern part of the GPS network covers the southern part of Nile Delta, whereas its eastern and western parts are deserts.

A campaign of observations has been repeated in the area each year between 1996 and 2000, except for 1997 where the observations have been repeated twice in January and October. The data length spans over five years that is long enough for obtaining reliable velocities at the observed sites [5]. GPS observations were collected using dual frequency Trimble 4000SSE and 4000SSI receivers. The sampling interval and elevation were fixed at 30 sec and 15°, respectively, throughout the survey.

The GPS data were organized into 24 hours segments covering a UTC day to facilitate the combination of the data with some of the surrounding IGS sites; ANKR, ONSA, KOSG, IISC, BAHR, YAR1, and MAS1 to constrain the site coordinates. Then, the data were processed using the GAMIT software, developed at MIT and SIO [6] to produce estimates and an associated covariance matrix of station position for each station with loose constrains on the parameters. To get a combined solution (site positions and velocities), all such covariance matrices are input to GLOBK, which is a Kalman filter. The basic algorithms and a description of this technique are given in [7] and its application to GPS data in [8]. By introducing global h-file, we have obtained

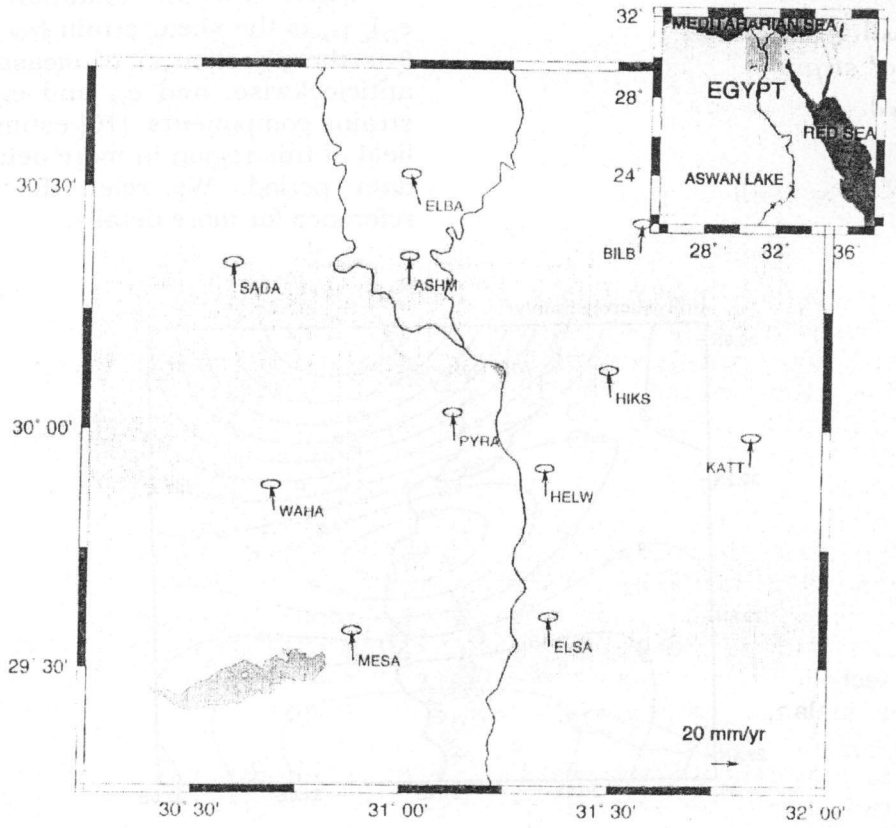

Fig. 1. Velocity field estimated by repeated GPS observations and its 95% confidence ellipses in ITRF96 reference frame for the period from 1996 to 2000 in and around Cairo city. The inset shows the location of Egypt and the studied region.

coordinates and velocity vectors at each site in the ITRF96 reference frame [9]. Fig. 1 shows the horizontal component of the velocity vectors with 95% confidence error ellipses. The horizontal components of these velocity vectors are further used to estimate the total strains by Least-Squares Prediction method. A detailed analysis of the GPS data is given in [10].

3. Total strains

First, the LSP technique to estimate the total strains using the GPS data was employed. The LSP method is a corollary of the Least-Squares Collocation (LSC) technique [11]. The application of this method to the crust deformation data was discussed in detail by [12, 13]. In this study, the total strain components were calculated following the method described by [13].

To estimate the total strains (elastic plus inelastic) in the GPS data for the period from 1996 to 2000, we used the horizontal velocity vectors shown in fig. 1. The average velocities were subtracted from all of the site velocities to remove the systematic bias. Then, the LSP were applied to each vector component (East-West and North-South) independently. The Empirical Covariance Function (ECF) for each component was fitted to the data [14]. Then, ECFs were used to reconstruct the displacement vectors (signal) at grid points of 7 km x 7 km mesh covering the studied region. Then, estimated velocities at this grid points were differentiated in space to obtain total crust strains. Figs. 2 and 3 are thus the estimated maximum shear strains, and principal axes of strains, respectively. The strain parameters were estimated in this analysis as follows [14]:

Maximum shear strain

$$\gamma_{max} = \{(e_{xx} - e_{yy})^2 + \gamma_{xy}^2\}^{0.5}.$$

Principal axes of strain

$\varepsilon_1 = 0.5\ (\Delta + \gamma_{max})$.

Principal axes of strain

$\varepsilon_2 = 0.5\ (\Delta - \gamma_{max})$.

Direction of ε_1

$\theta = 0.5 \tan^{-1} \{\gamma_{xy} / (e_{xx} - e_{yy})\}$.

Where Δ is the dilatation strain ($\Delta = e_{xx} + e_{yy}$); γ_{xy} is the shear strain $\{\gamma_{xy} = 0.5\ (e_{yx} + e_{xy})\}$; θ is the direction ε_1 of measured from x-axis anticlockwise; and e_{yx} and e_{xy} are the linear strains components. [10] estimated the strains field of this region in more details for the same data period. We refer the reader to this reference for more details.

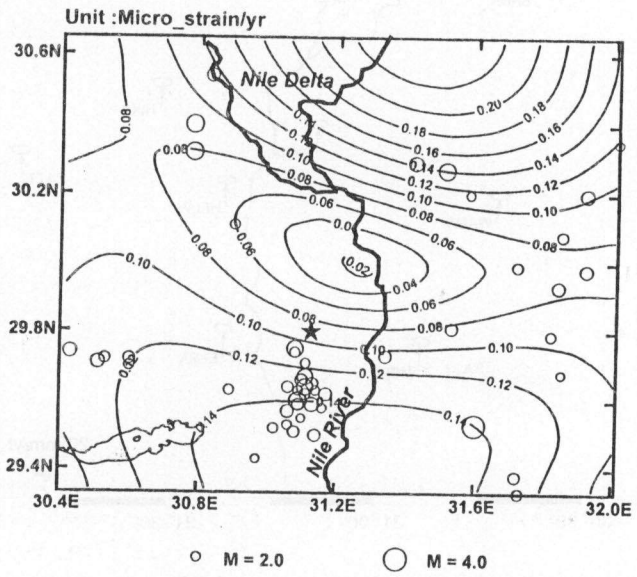

Fig. 2. Distribution of the maximum shear strain rates in the Greater Cairo region estimated by the LSP technique for the period from 1996 to 2000. Unit is μ strain/yr. Shallow earthquakes (d<30 km) of magnitude greater or equal to 2.0 from Jan. 1996 to Dec. 2000 are plotted (Egyptian Seismic Network and ISC).

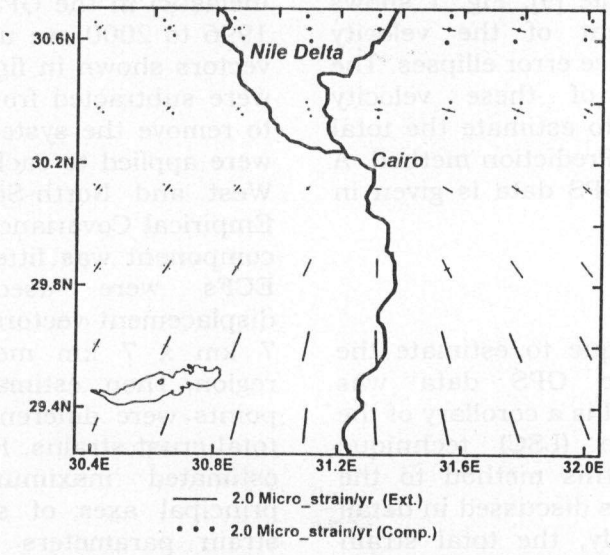

Fig. 3. Magnitude and orientation of principal axes of strains in the Greater Cairo region estimated by the LSP technique for the period from 1996 to 2000. Dashed lines are compression strains and straight lines ones are extensional strains, respectively. Unit is μ strain /yr.

4. Inelastic strains and inversion analysis

Ref. [4] proposed a formulation of an inverse problem relating surface deformation and inelastic properties of the earth's crust. They showed that, the inelastic properties of the crust could be studied if its deformation is measured. In this section we will make use of their hypothesis to isolate the inelastic properties of the Cairo region so that reliable crust strains can be delineated for earthquake prediction studies.

The elasto-plastic constitutive relations of the heterogeneous earth's crust are expressed in terms of stress and strain as,

$$\sigma_{ij} = C_{ijkl}(\varepsilon^R_{kl} - \varepsilon^P_{kl}). \quad (1)$$

Where C_{ijkl} is the stress tensor, ε^R_{kl} is the observed (total) strain increment, and ε^P_{kl} is the plastic (inelastic) strain increment or eigen strain. From eq. (1) the observed stress, σ^R_{ij}, and plastic stress, σ^P_{ij}, can be expressed in the following forms;

$$\sigma^R_{ij} = C_{ijkl}\,\varepsilon^R_{kl} \quad \text{and} \quad \sigma^P_{ij} = C_{ijkl}\,\varepsilon^P_{kl}, \quad (2)$$

σ^P_{ij} is usually called eigen stress or polarized stress. When eigen stress =0, then the material is fully elastic, i.e., $\sigma_{ij} = \sigma^R_{ij}$. We can rewrite eq. (1) in the following form;

$$\sigma_{ij} = \sigma^R_{ij} - \sigma^P_{ij}. \quad (3)$$

By space differentiation of eq. (3) with respect to x and y, respectively, we get the following equations;

$$\sigma_{11,1} + \sigma_{12,2} = \sigma^R_{11,1} + \sigma^R_{12,2} - \sigma^P_{11,1} - \sigma^P_{12,2}, \quad (4)$$

$$\sigma_{21,1} + \sigma_{22,2} = \sigma^R_{21,1} + \sigma^R_{22,2} - \sigma^P_{21,1} - \sigma^P_{22,2}. \quad (5)$$

Where, the subscripts 1 and 2, following the comma in the above equations stand for the derivatives with respect to x and y, respectively. From the equilibrium condition, the left hand side of eqs. (4) and (5) should be equal to zero. Then, we have;

$$\sigma^P_{11,1} + \sigma^P_{12,2} = \sigma^R_{11,1} + \sigma^R_{12,2}, \quad (6)$$

$$\sigma^P_{21,1} + \sigma^P_{22,2} = \sigma^R_{21,1} + \sigma^R_{22,2}. \quad (7)$$

Here we assume that plastic strain increment does not have volumetric part (ε^P_{ii} =0), which means $\varepsilon^P_{11} + \varepsilon^P_{22} = 0$ and $\varepsilon^P_{33} = 0$.

Once again, by differentiation of eqs. (6) and (7) with respect to x and y, respectively and considering the above assumption, we can get the following equations;

$$\sigma^P_{11,11} + \sigma^P_{11,22} = \sigma^R_{11,11} - \sigma^R_{22,22}, \quad (8)$$

$$\sigma^P_{12,11} + \sigma^P_{12,22} = \sigma^R_{12,11} + \sigma^R_{12,22} + \sigma^R_{11,12} + \sigma^R_{22,12}. \quad (9)$$

Eqs. (8) and (9) are therefore our target to solve the inverse problem;

The inverse problem then reduces to a pair of Poisson equations as follows;

$$\sigma^P_{11,11} + \sigma^P_{11,22} = \rho_1(x, y),$$
$$\sigma^P_{12,11} + \sigma^P_{12,22} = \rho_2(x, y). \quad (10)$$

The source terms of the above Poisson's equations are known. Then, straightforward by the Finite Difference Equations (FDE) technique [15], eq. (10) can be solved for the inelastic normal and shear strains. Finally, the maximum shear of inelastic strain is given by;

$$\sigma^P_{max} = \{(\sigma^P_{11} + \sigma^P_{22})^2 + (\sigma^P_{12})^2\}^{1/2}. \quad (11)$$

The right hand side of eqs. (8) and (9) gives us the known surface deformation and the left hand side gives us the unknown inelastic properties of the crust. The known surface deformations are the first and second partial derivatives of the total strains at each grid point estimated in section 3.

5. Results and discussions

Fig. 4 shows the estimated maximum shear rates of the inelastic strains in and around Cairo City. The obtained inelastic shear strain rate does not exceed 1.0×10^{-8}/yr everywhere in the studied region. Although the magnitude of the inelastic strain rate is very small, it is significant especially in the patched areas as shown in fig. 4. The uncertainty is

estimated to be in the range of 25-45% of the obtained inelastic strains.

Maximum shear inelastic strains, fig. 4, show two patches of relative inelasticity in the Northern and Southern parts of the studied region. In addition, there is a low inelastic strains zone in the middle of the region. The epicenters of shallow earthquakes of depth less than 30 km that occurred in the same interval of GPS data are plotted in fig. 4 to compare the inelasticity with the seismic data. It should be noted that, the inelastic strain field in these two high regions might not relate to any co-seismic and/or post-seismic movements. The seismicity of these regions was low during the studied period, as it will be mentioned later. Since the increase in the inelastic strains (plasticity) might indicate the eminence of an earthquake faulting in the studied area, there is a possibility for seismic activity in the northern and southern parts of the studied area where the inelastic strain rates are relatively high.

A closer look at figs. 3 and 4 suggests that, there is a spatial correlation between inelastic and total strains in the northern and southern regions, but slightly shifted to the eastward direction. Since this is a unique example in this region so far, it is very difficult to say whether it just a coincidence or tectonically possible phenomena. However, generally the inelastic strain rates over the studied region, fig. 4 are very low (10^{-3} μstrain/yr) compared to the total rates (10^{-1} μstrain/yr) fig. 3. This suggests that, the Cairo region deforms mostly elastically, and the crust stresses at surface can be well explained by the simple elasticity theory, as it will be discussed later.

The above inversion technique introduced in this study can be applied in other active areas in Egypt, such as Aswan area or Red Sea area as a possible criterion for forecasting of large inland earthquakes because, as it is mentioned above, the increase in the inelastic strains (plasticity) might indicate the eminence of an earthquake faulting.

Based on the above analysis, we may conclude that the Cairo region deforms mostly elastically and that figs. 2 and 3 represent the elastic crust-strains of the present interval. On the other hand, the crust stresses at the surface were estimated by the simple elasticity theory as shown in figs. 5 and 6. In this analysis, the Poisson's ratio and rigidity are assumed to be 0.25 and 0.5×10^{11} N/m^2, respectively. Although the maximum shear stress, fig. 5, and principal axes of stress, fig. 6, estimated based on the elasticity theory and from only five years of data, they well portray characteristics of the tectonic deformation in the Cairo region.

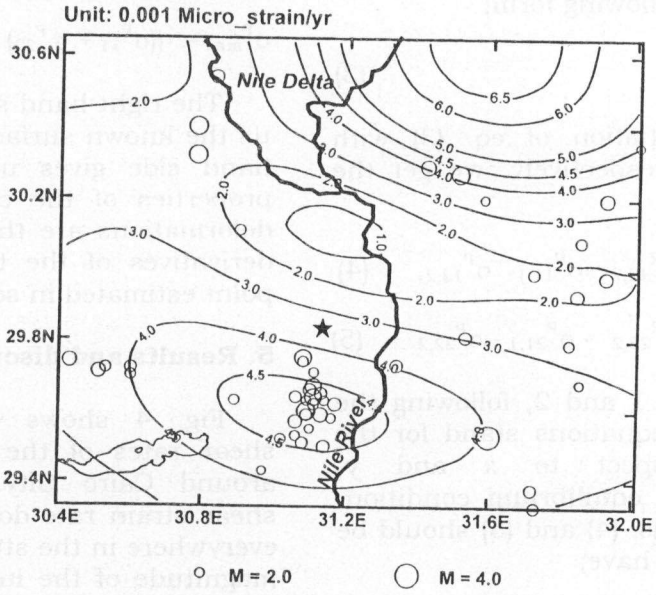

Fig. 4. Distribution of the rate of the maximum shear inelastic strains in and around the Cairo City as estimated by LSP and FDE for the period from 1996 to 2000. Unit is μstrain/yr. Epicenters of shallow earthquakes (d≤ 30 km) are plotted.

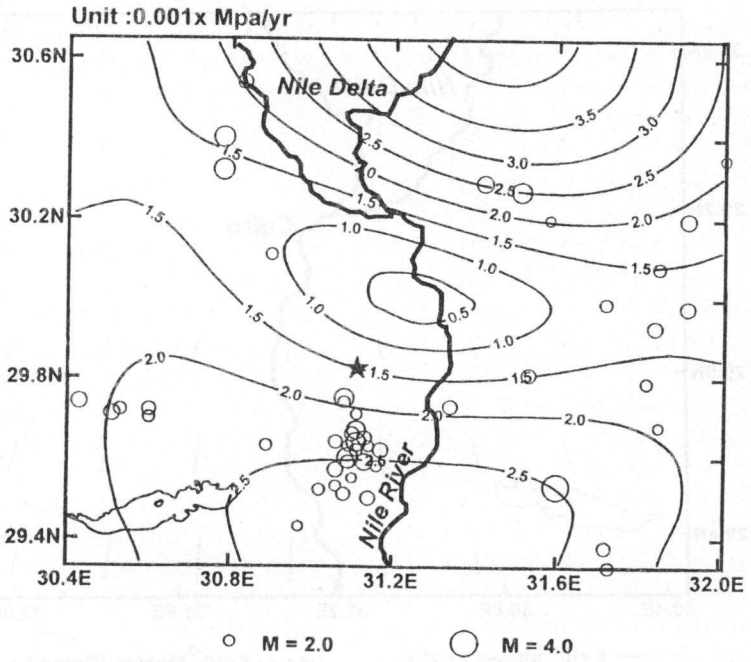

Fig. 5. Distribution of the maximum shear stress rates in and around the Cairo City as estimated by LSP and FDE for the period from 1996 to 2000. Unit is 0.001 MPa/yr. Epicenters of shallow earthquakes (d≤ 30 km) are plotted.

Since the crust shear stresses are estimated based on the elastic theory, they showed the same patterns of the elastic strains shown in figs. 2 and 3. The pattern of maximum shear stresses, fig. 5, show two maxima of high values of stress in the northern and southern areas separated by a very low stress or almost stress-free zone in the middle of the region. It is interesting to note that, at the southern edge of the above low area, the October 12, 1992 earthquake occurred, fig. 6. We should also note that the first GPS campaign was in 1996, about four years after the October 1992 earthquake. Therefore, we may able to say that the accumulated stresses in this low zone were almost released by the co-seismic and the post-seismic of the October 1992 earthquake. In addition, the present analysis shows that there is no any evidence for earthquake activity in this low zone in the near future. However, there is still possibility for seismic activity in the northern or southern parts of the studied area where the stresses rate are relatively high. The rate of maximum shear stress found to be maximum in the northern and southern areas of the study region (4.2×10^{-3} MPa/yr), which might be due to the subduction of the African plate under the Eurasian plates and the tectonic motion along the Gulf of Suez as well as the deformation along the NW-SE and W-E faults [10] in the region. On the other hand, the Maximum shear stresses in the two maxima in northern and southern areas may not relate to any co-seismic and/or post-seismic movements. The seismicity of this area was very low during the period of our interest; with the largest magnitude of earthquake being recorded was less than 4.5. Also, to compare the maximum shear stresses with the seismic data, epicenters of shallow earthquakes are superimposed on fig. 6. The above low zone of stresses has been confirmed by seismic data. [16] used the seismic data for the period 1910-1999 and [17] to estimate the earthquake energy release as function of time and location in and around the Cairo city. His results showed that the level of earthquake activity is very low throughout the studied region, except for the Dahshour area for the period 1992-1993.

The distribution of principal axes of stresses, fig. 6, shows a general contraction of about 8.2 MPa/yr in nearly north-south direction in the northern part of the studied

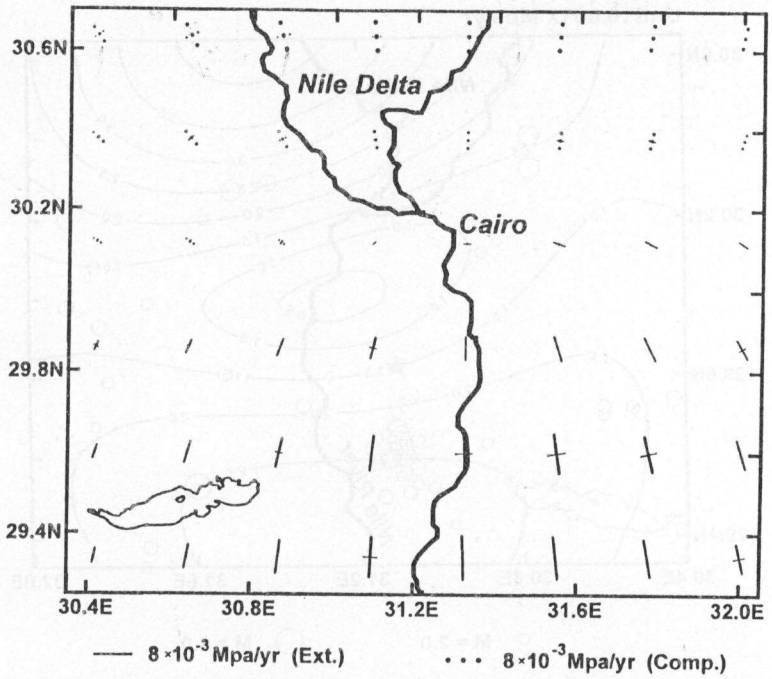

Fig. 6. Magnitude and orientation of principal axes of elastic stresses in and around the Cairo City as estimated by LSP and FDE for the period from 1996 to 2000. Unit is 0.001 MPa/yr.

region. This may be due to the compression force acting at the convergent plate boundary between the Eurasian and the African plates. The present analysis indicates that the effect of this force might be extended to the southern part of the Nile Delta. In addition, the large area of extensional stresses in the southern part of the area, fig. 5, seems in relation with the tectonic motion along the Gulf of Suez and the deformation along the NW-SE and W-E faults in this region [10]. On the other side, the direction of compression stresses derived in this study for the Cairo region from GPS is in a good agreement with that deduced from earthquake focal mechanisms and borehole breakouts by [18].

Generally, the low maximum shear stress rates and low level of earthquake occurrence in the central part of the studied region (the low zone) during the present interval indicate that internal deformation in this region is very small.

Finally, we can say that the Cairo earthquake of 12 October 1992 rings an alarm for the future urban strategy in Egypt. To mitigate the effects of similar future disastrous earthquakes, seismic risk factors should be considered. On the other hand, monitoring the crust stress/strain perturbations is a key to understand the physical process in the crust to forecast the crust activity. A continuous GPS tracking network supplemented by a dense seismic network could provide us with one of the ideal tools to realize this. For this purpose the National Research Institute of Astronomy and Geophysics (NRIAG) have installed a modern seismic network and planning to establish a continuous GPS tracking network in Egypt.

5. Conclusions

The velocity vectors in ITRF96 obtained from six GPS campaigns during 1996-2000 have been used to estimate the elastic strains and inelastic properties in and around the Cairo City. Least-squares prediction method to estimate the total strains in the data period, were firstly applied. Then, inelastic strains of the studied area have been estimated using the inversion technique introduced by [4]. The resultant rate of inelastic strain is in the order of 10^{-2} μstrains/yr. When compared with the rate of total strain of the order of 0.1

μstrains/yr, non-elastic part of strains may be negligible (less than 1.0 %). This suggests that Cairo region deforms mostly elastically, and the crust stresses at the surface can be well explained based on the simple elastic theory. A compression stress regime is observed in the northern part of the studied region, which might be due to the collision of Africa and Eurasia. The relatively large area of stresses strains in the southern part of the studied region may be related to the tectonic motion along the Gulf of Suez and the deformation along the NW-SE and W-E faults in the region. Maximum shear stresses show two maxima of high values of stress in the northern and southern parts of the studied region separated by a very low zone of maximum shear stresses or almost stress-free zone in the middle of the region. At the southern edge of this low area, the October 12, 1992 earthquake occurred. This indicated that the accumulated strain in this low zone was totally released by the co-seismic and the post-seismic of the October 1992 earthquake. In addition, the present analysis shows that there is no evidence for earthquake activity in this low zone in the near future. This low zone of stresses has been confirmed by seismic data.

Acknowledgments

The author is very grateful to the staff of National Research Institute of Astronomy and Geophysics, Helwan, Cairo, who collected the field GPS data. He also thanks Prof. Ali Tealeb for his kind help and useful discussions.

References

[1] H. E. Abdel Hafiez, The Role Of Earthquake Analysis For Modeling The Crustal Structure And Constructing Local Magnitude Scale. M. Sc. thesis, Ain Shams Univ., Faculty of Science (1995).

[2] A. Badawy, and P. Monus, "Dynamic source parameters of the 12th October Earthquake, Cairo, Egypt," J. Geodyn., Vol. 20 (2), pp. 99-109 (1995).

[3] A. El-Sayed, R. Arvidsson, and O. Kulhanek, " The 1992 Cairo earthquake: A case study of a small destructive event," J. of Seismology, Vol. (2), pp. 293-302 (1998).

[4] M. Hori, T. Kameda, and N. Hosokawa, "Formulation of identifying material property distribution based on equivalent inclusion method", J. Struct. Mech. Earthquake Eng., JSCE, Vol. 619, pp. 1-47 (1999).

[5] T. Kato, G. S. El-Fiky, E. N. Oware, and S. Miyazaki, "Crustal Strains In The Japanese Islands As Deduced From Dense GPS Array," Geophys. Res. Lett., Vol. 25, pp.3445-3448 (1998).

[6] R. W. King, and Y. Bock, Documentation for the MIT GPS Analysis Software. Mass. Inst. of Techno., Cambridge (1991)

[7] T. A. Herring, J. L. Davis, and I. I. Shapiro, "Geodesy by Radio Interferometry: The Application of Kalman Filtering To The Analysis of Very Long Baseline Interferometry Data," J. Geophys. Res., Vol. 95, pp.12561-12581 (1990).

[8] K. L. Feigl, R. W. King, T. A. Herring, and M. Rothacher," Space Geodesy Measurement of Crustal Deformation In Central and Southern California 1984-1992," J. Geophys. Res., Vol. 98, pp.21677-21712 (1993).

[9] C. Boucher , Z. Altamimi and P. Sillard, Resultas analysis of the ITRF 96. IERS technial note 24, observatory de Paris, (1998).

[10] G. S. El-Fiky, A. Tealeb, M. Rabah, A. Mousa, K. Zahran, and A. Raiyan, "Present-day crustal deformation in and around the Cairo City, Egypt, as derived from GPS measurements and its tectonic implications". (Submitted) Bull. National Research Institute of Astronomy and Geophysics, Helwan, Cairo, Egypt (2002)

[11] H. Moritz, "Interpolation and prediction of gravity and their accuracy. Report No. 24, Inst. Geod. Phot. Cart. The Ohio State Univ., Columbas, USA (1962).

[12] G. S. El-Fiky, T. Kato and Y. Fujii, "Distribution Of The Vertical Crustal Movement Rates In The Tohoku District, Japan, Predicted By Least-Squares Collocation," J. Geodesy, Vol. 71, pp.432-442 (1997).

[13] G. S. El-Fiky, and T. Kato, "Interplate Coupling In The Tohoku District, Japan, Deduced From Geodetic Data Inversion".

J. Geophysical Research, Vol. 104, 20,361-20,377 (1999a).

[14] G. S. El-Fiky, and T. Kato, "Continuous Distribution of The Horizontal Strain in The Tohoku District, Japan, Deduced From Least Squares Prediction. J. Geodynamics," Vol. 27, pp.213-236 (1999b).

[15] R. D. Richtmyer, and K. M. Morton, "Difference methods for initial value problems", New York: Wiley-interscience (1967)

[16] A. S. Mohamed, "Seismicity And Recent Crustal Movement Studies in And Around The Greater Cairo Region, Egypt, "Acta. Geod. Geoph. Hung., Vol. 36 (3), pp.353-362 (2001).

[17] C. F. Richter, Elementary seismology. W H Freeman Company, San Francisco, California (1958)

[18] A Baodawy, the present-day stress field in Egypt. Annalidi Geofisica, Vol. 44 (3), pp. 557-570 (2001).

Received January 22, 2002
Accepted April 22, 2002